

Jupiter's Great Red Spot: A Study of Vortex Dynamics

PHY1530 Final Report

Tanisha Ghosal

December 19, 2023

Abstract

Studying the atmospheres of other planets is a significant area of planetary science research; it allows for insights into how factors like atmospheric composition, distance from the host star, and planet size can give rise to a variety of climates. Jupiter and other gas giants exhibit complex atmospheric phenomena, one of the most prominent being the Great Red Spot (GRS), a massive and persistent anti-cyclonic storm on Jupiter. This report first explores fundamental questions in the field of planetary science and motivates the study of the GRS, before discussing the vortex dynamics that govern it. These dynamics are discussed in the context of two studies. The first, by Philip (1993), explores the mathematical derivation of quasi-geostrophic theory, and how it can explain the prograde vortices that give rise to the persistent nature of the GRS. The second study, by Sánchez-Lavega et al. (2018), discusses how the cloud morphologies within the GRS can be inferred and characterized from images taken by JunoCam, a camera aboard the Juno spacecraft. The key results of both of these studies are presented in this report, outlining various aspects of the GRS that are active areas of research. At the end of this report, the results of a simulation are shown. This simulation is based on the shallow water approximation, a simple model (valid when the horizontal scale is much larger than the vertical) for how vortices interact in the Jovian atmosphere. The overall objective of this report is to provide a comprehensive view into how the GRS developed, how it continues to persist, and how we can learn more about it through mathematical theory, data analysis, and numerical simulations.

1 Introduction

Gas giants such as Jupiter are often characterized by the swirling movement of gases in their atmospheres. These movements lead to the formation of structures called vortices, which are regions of rotating fluid. The formation of vortices on gas giants is thought to be driven by a combination of factors, including the rotation of the planet, the variation in temperature and pressure across the atmosphere, and the composition of gases. One of the most famous vortices is Jupiter's Great Red Spot (GRS), shown in Figure 1. It is a massive, persistent anti-cyclonic storm that has been observed for centuries by spacecraft such as Voyager 1 & 2, the Hubble Space Telescope, and Juno. The GRS is known to be the largest observed storm in the solar system, and has been the subject of many scientific studies. This report will present the results of two such studies: the vortex dynamics theory of the GRS presented in the review paper by (Philip, 1993), and the discussion of the dynamics inferred by JunoCam images reported by (Sánchez-Lavega, et al, 2018). This report will additionally present findings from a simulation of the shallow water model, illustrating the complexities of large-scale vortex simulations and drawing parallels to the dynamics observed in Jupiter's Great Red Spot.



Figure 1: The Great Red Spot on Jupiter, a significant and persistent anti-cyclonic storm. (Credit: NASA, Juno.)

1.1 Significance

Prior to discussing the GRS in greater detail, it's imperative to discuss the motivation for studying planetary atmospheres, major questions in the field, and the specific research outlined by the two papers. Planetary atmospheres serve as natural laboratories to study how different conditions – such as atmospheric composition, distance from the host star, and planet size – can give rise to a variety of climates. Jupiter, being the largest planet in our Solar System, offers a unique opportunity to investigate extreme conditions not found on Earth. The mechanisms that govern Jupiter's atmosphere, from the complex weather patterns, distinct cloud formations, to the massive storm systems like the GRS, are not well understood. Studying the GRS increases our understanding of how fundamental fluid mechanics quantities, such as vorticity and shear, interact and evolve to form various atmospheric structures. Below are some major questions specific to Jupiter and the GRS:

- Can an enhanced understanding of the roles played by physics and chemistry in shaping planetary climates, such as Jupiter's, provide deeper insights into Earth's climate change? (National Research Council, 2011)
- What is the distribution of gases within the Great Red Spot, both vertically and horizontally, and how do variations in temperature and internal dynamics contribute to the structural features of this storm?
- By what mechanisms has the Great Red Spot managed to endure for centuries, and what underlying factors contribute to its longevity within Jupiter's turbulent atmosphere?

The selected papers address questions more specific to the GRS. In Philip (1993), the main questions are: How do vortices manifest in Jupiter's turbulent atmosphere? What sets the scale of the vortices? How do vortices merge together? These questions are answered through the discussion of the quasi-geostrophic approximation and the equations governing the circulation of vortices. In Sánchez-Lavega, et al (2018), the main question is: How can we learn more about the dynamics of the GRS from images produced by Juno? This question is answered through comparisons between these images and those from prior studies to analyze how cloud morphologies of the GRS can provide insight into the dynamics within them.

2 Results

The following subsections will explore the results of (Phillip, 1993) and (Sánchez-Lavega, et al, 2018).

2.1 Vortex Dynamics Theory in (Philip, 1993)

Golitsyn (1970) was the first to suggest that the GRS is not attached to any topographic feature, and Ingersoll & Cuong (1981) argued that the GRS is quasi-geostrophic and maintains itself by merging with and absorbing smaller vortices. Geostrophic motion pertains to winds that arise from a precise equilibrium between the Coriolis force and horizontal pressure-gradient forces. In contrast, quasi-geostrophic (QG) motion describes flows where the Coriolis force and pressure gradient forces are nearly balanced, with inertia also playing a role. The following subsections will first discuss preliminary equations, and then delve into the quasi-geostrophic approximation.

2.1.1 Vorticity

Vorticity is a fundamental concept in fluid mechanics that describes the local rotation of fluid elements in a flow. In its simplest form, vorticity is the curl of the velocity vector of a fluid particle. Taking the curl of the Navier Stokes equation generates the following (for ideal flow), where $\frac{D}{Dt}$ is the material derivative:

$$\frac{\partial \omega}{\partial t} = \nabla \times (\mathbf{u} \times \omega) \quad (1)$$

$$\frac{D\omega}{Dt} = \omega \cdot \nabla \mathbf{u} \quad (2)$$

For non-zero viscosity,

$$\frac{D\omega}{Dt} = \omega \cdot \nabla \mathbf{u} + \nu \nabla^2 \omega \quad (3)$$

2.1.2 Quasi-Geostrophic Approximation

When analyzing fluid motions within a thin atmospheric shell where the vertical extent is significantly smaller than the horizontal, it is customary to depict the shell as a linked series of thin layers while disregarding the atmosphere both above and below the shell. If we assume that the density of the atmosphere increases rapidly with depth such that the fluid below the shell is not affected by motions in the shell, we can parameterize the thickness of a single layer of fluid as $H = H_0 + h(x, y, t) - h_b(x, y)$. This rough approximation works well when the characteristic vorticity of the flow is small compared with the angular velocity of the rotating planet, the surfaces of constant density and pressure are coincident (small baroclinic forces), and the horizontal scales are larger than the vertical (these are all true for Jupiter!) This model is referred to as the one-layer shallow water approximation. The horizontal component of the angular momentum in this approximation:

$$\frac{D\mathbf{v}}{Dt} \equiv \frac{\partial \mathbf{v}}{\partial t} + (\mathbf{v} \cdot \nabla \mathbf{v}) = -g \nabla h + f(y) \mathbf{v} \times \hat{\mathbf{z}} \quad (4)$$

where g is the reduced acceleration of gravity, $\hat{\mathbf{z}}$ is the unit vector in the vertical direction, and $f(y)$ is the Coriolis parameter which is defined to be double the magnitude of the planet's angular velocity component in the $\hat{\mathbf{z}}$ direction. The other equation that governs the dynamics is the continuity or mass-conservation equation. By combining it with the curl of Equation 4, it can be written as (Ghil & Childress 1987):

$$\frac{D\mathbf{v}}{Dt} = \left(\frac{\omega(x, y, t) + f(y)}{H} \right) = 0 \quad (5)$$

where $\omega(x, y, t) = (\nabla \times \mathbf{v}) \cdot \hat{\mathbf{z}}$ is the vertical component of the vorticity. The potential vorticity is also defined as $q = H_0[w(x, y, t) + f(y)]/H$. A simpler case occurs when f and H are constant, so 5 becomes $\frac{D\omega}{Dt} = 0$, this is the curl of Euler's equation. One of the solutions for this equation is the point of circulation: $\Gamma : \omega(x, y, t) = \Gamma \delta(x - x_0) \delta(y - y_0)$, and the velocity due to the vorticity can be found by the Biot-Savart law, $\frac{d\mathbf{x}}{ds} = |\boldsymbol{\omega}|[\mathbf{x}(s)]$, where x denotes the vector cross product. For a single point vortex, the velocity of the vortex is zero, implying there is no self-advection and that the vortex remains at rest. A collection of N point vortices that have,

$$\omega(x, y, t) = \sum_{i=1}^N \Gamma_i \delta[x - x_i(t)] \delta[y - y_i(t)] \quad (6)$$

is also a solution to $\frac{D\omega}{Dt} = 0$, where the circulations of the vortices Γ_i remain constant and the guiding centres of each vortex $[x_i(t), y_i(t)]$ move with the local velocity (Chorin, 1993). As an example, two point vortices of the same sign rotate about their centre of vorticity, whereas a dipolar pair of vortices with strengths $\pm\Gamma$ and separation d advect in the direction perpendicular to the line between them, at a velocity of $\Gamma/2\pi d$. The GRS consists of many vortices, so understanding how numerous vortices of different polarities interact is of great importance.

A small problem is that Equation 5 is not advectively linear (ω is not linearly related to \mathbf{v}). However, we can use the quasi-geostrophic (QG) approximation to make it advectively linear, and to easily interpret the solutions physically. The approximation scales the velocity (v), the characteristic horizontal length (l), the vorticity (ω), and the Coriolis parameter ($f(y)$) such that depend on the Rossby number, $\epsilon = v/lf(y)$. To leading order in ϵ , the QG momentum equation becomes the kinematic geostrophic balance equation:

$$\mathbf{v} = \hat{\mathbf{z}} \times \nabla \left(\frac{gh}{f_0} \right) \equiv \hat{\mathbf{z}} \times \nabla \psi \quad (7)$$

In this approximation, $(\nabla \cdot \mathbf{v}) \equiv 0$ and \mathbf{v} can be found from the streamfunction $\psi = gh/f_0$. The equation for the potential vorticity,

$$\frac{D}{Dt} \left\{ \omega + [f(y) - f_0] - \frac{hf_0}{H_0} + \frac{h_b(x, y)f_0}{H_0} \right\} = \frac{D}{Dt} \left\{ \nabla^2 \psi - \frac{\psi}{L_r^2} + \frac{h_b(x, y)f_0}{H_0} + [f(y) - f_0] \right\} = 0 \quad (8)$$

where f_0 is the average value of $f(y)$ at the given latitude and L_r is the Rossby deformation radius found as $\sqrt{\frac{gH_0}{|f_0|}}$.

This equation can be decomposed by breaking the velocity into the sum of a time-independent and x -independent zone belt-part $\bar{\mathbf{v}} = \bar{\mathbf{v}}_{\mathbf{x}} \hat{\mathbf{x}}$, and a time-dependent remainder $\tilde{\mathbf{v}}(x, y, t) \equiv \mathbf{v}(x, y, t) - \bar{\mathbf{v}}$. If we define \tilde{q} , the potential vorticity when $\mathbf{v} = \bar{\mathbf{v}}$, and define $\tilde{q}(x, y, t) = q - \bar{q}$, we can write an advectively linear and homogeneous equation:

$$\frac{D\tilde{q}}{Dt} = \left[\frac{\partial}{\partial t} + (\tilde{\mathbf{v}} \cdot \nabla) + \bar{\mathbf{v}} \frac{\partial}{\partial x} \right] (\nabla^2 \tilde{\psi} - \tilde{\psi}/L_r^2) = 0 \quad (9)$$

In this case, $\tilde{\mathbf{v}}(x, y, t)$ represents the coherent vortices, the turbulent component of the flow, and the Rossby waves (the latter being the movement of air due to Jupiter's rotation). This equation allows for the classification of vortices, one of the major ones being whether they are prograde or adverse. The potential vorticity \tilde{q} and the local zone-belt shear $\bar{\sigma}(y) = \frac{-\partial \bar{v}_x}{\partial y}$ are defined as adverse if they have opposite signs, otherwise, they are prograde. Adverse and prograde vortices evolve differently in shape and directionality, and numerical simulations show that prograde vortices are able to relax to stable equilibria. Prograde vortices are supported by QG theory (Marcus, 1988), and are additionally confirmed by the shear found from Voyager observations. Another classification of vortices from this equation is whether they are corner-like or band-like. When vortices become linearly unstable before reaching their limiting solutions, they are corner-like, whereas they are band-like vortices if they never reach the region of adverse shear. The GRS is a "hybrid" of these, with the equatorial side of the anti-cyclones acting corner-like and the pole side band-like. Overall, the QG equations can be used to classify vortices and understand how they scale, merge, and give rise to the turbulence within the GRS.

2.2 JunoCam Image Analysis in (Sánchez-Lavega, et al, 2018)

Employing high-resolution images captured by JunoCam aboard the Juno spacecraft during its close encounter with Jupiter on July 11, 2017, this study conducts an analysis of GRS dynamics at the upper cloud level. The study measures the horizontal velocity and vorticity fields, utilizing clouds as tracers to track the flow patterns. Although JunoCam was primarily intended to take images used for public outreach, the images can also be processed for scientific purposes. JunoCam obtained images with filters Blue (480.1 nm), Green (553.5 nm), and Red (698.9 nm), which were combined to compose colour images on a cylindrical map projection, as shown in Figure 2.

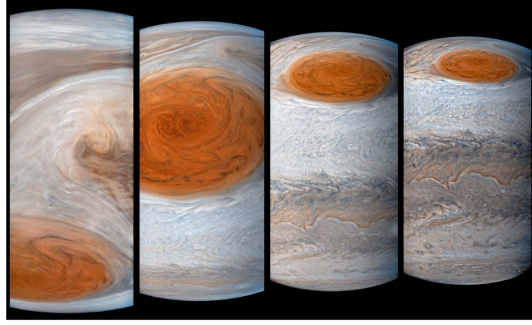


Figure 2: RGB Images of GRS on July 11, 2017, generated by G. Eichstadt and J. Cowart (Credit: Sánchez-Lavega, et al, 2018)

The winds were measured from these images by either manually tracking the clouds and retrieving the zonal and meridional velocities from fitting the longitude and latitude drifts, or using image-correlation software to identify cloud motions. After creating a composite of these images, they were able to find the velocity field within the GRS through the use of image-correlation velocimetry, and the vorticity field from the wind field by using $\zeta = -\frac{1}{R} \frac{\partial u}{\partial \phi} + \frac{u}{r} \sin \phi + \frac{1}{r} \frac{\partial v}{\partial \lambda}$, derived in Dowling & Ingersoll, 1988. They found no noticeable changes in the wind field velocity and vorticity, but were able to identify several dynamical regions due to the cloud morphologies, shown in Figure 3.

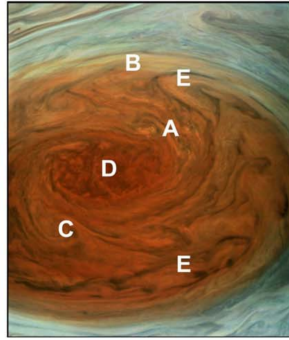


Figure 3: JunoCam regions with dynamical regions labelled: (A) compact cloud clusters; (B) mesoscale waves; (C) spiralling vortices; (D) a central turbulent nucleus; (E) elongated thin dark gray filaments, (Credit: Sánchez-Lavega, et al, 2018)

They found that dynamical region A resembles altocumulus clouds on Earth, where cellular moist convection is driven by a Rayleigh-Benard convective instability (Houze 2014). On Jupiter, this convection would involve ammonia or water vapour as sources of heat that warm ascending parcels to form cumulus clouds. Dynamical region B consists of mesoscale waves that could be gravity waves or shear instability waves, depending on the Richardson number $Ri = N^2/(du/dz)^2$, where N is a characteristic frequency and du/dz is the vertical shear of the zonal wind. Dynamical zone C is an anti-cyclonic vortex (high-pressure centre, air moves apart and sinks), and has been difficult to reproduce in numerical simulations due to required approximations of the horizontal wind velocity. The central nucleus, dynamical region D, has cloud morphologies that suggest the presence of three coupled weak circulations, but the data quality prohibits the confirmation of results from (Liu et al, 2012), which imply that there is a central source of spiralling streamlines. Lastly, dynamical region E are dark grey filaments in the outer part of the GRS, it is not clear whether they are traced by darker aerosols or represent areas of different altitudes and particle densities. The authors suggest that these are possibly Rossby waves, which are important for hurricanes on Earth (Montgomery & Kallenbach, 1997).

3 Discussion

In Philip (1993), the quasi-geostrophic approximation was explained in detail to illustrate why it is effective at describing the GRS. One of the main conclusions from the theory is that a vortex with uniform potential vorticity and radius greater than the Rossby deformation radius L_r has a quiet centre, with most of the vorticity and velocity being concentrated in a thin ring at the vortex's outer edge. This is true for the GRS, where the vorticity is measured to be near zero at the centre, rises to its peak value of $3 \times 10^{-5} s^{-1}$ at the inside edge of the ring, and decays to zero outside the GRS. Even after Voyager observations demonstrated that the vorticity and circumferential velocity of the GRS increased rapidly away from its centre, an exponential dependence on distance was not attempted until 1988. This is where the QG approximation came in, because unlike other approximations (such as the intermediate-geostrophic (IG) approximation), it models the vorticity profile of the GRS as an exponential. Another source of disagreement between the approximations is that IG predicts that anti-cyclones are preferred over cyclones, whereas QG predicts about equal numbers of anti-cyclones and cyclones. Based on observations, it seems that there are more anti-cyclones on Jupiter (agreeing with IG), but this could be attributed to the fact that cyclones may be overlooked in Voyager images because the clouds are filamentary and diffuse, and therefore harder to see.

Overall, while acknowledging the presence of non-QG components in Jovian vortices, the paper discusses that QG theory provides a robust framework for understanding their properties. Notably, Jovian vortices exhibit prograde motion irrespective of their cyclonic or anti-cyclonic nature, and are the reason for the large, weakly dissipative (long-lasting) vortices in the GRS. The size of QG vortices is determined by the widths of the zones in which they lie, although the loss of stability and flattening that lead to merging depends on L_r , and whether the vortices are band-like or corner-like. The classification of vortices from QG theory (such as whether they are prograde vs. adverse, corner-like vs. band-like) therefore answers many of the questions that the paper sought to answer – such as what sets the scale and shape of the GRS and why the GRS continues to persist. Lastly, the paper calls for further research, especially in developing a self-consistent model accounting for both east-west winds and thermal convection, for a more comprehensive understanding of the GRS.

In Sánchez-Lavega, et al (2018), the authors detail the calibration assumptions of JunoCam (mounting, optics, and distortion coefficients) and described the methods used for image processing. The composite image formed from tracking wind measurements allowed them to identify and analyze various features within the GRS, such as compact cloud clusters, mesoscale waves, internal spiralling vortices, the central nucleus, and large dark thin filaments. The authors then describe the potential sources of each of these features, along with comparisons with findings from other studies to validate their findings. In these comparisons, they found that there is a hightemporal variability in the dynamics of this layer, strongly enforced by the interaction of the GRS with phenomena close in latitude. This was supported by the peaks in wind field and vorticity patterns found at various latitudes. The study also notes that while the GRS has changed significantly in the past 140 years (Rogers 1995), the wind field in the GRS shows slight changes during 1979–2017, implying a deeply-rooted circulation. Overall, the wind and cloud analysis in this paper offers valuable insights into the turbulent atmosphere that sustains the GRS, and answers the research question of what we can infer about the GRS from images of Jupiter.

4 Conclusion

In conclusion, this report explored the vortex dynamics of the GRS by analyzing the insights from the quasi-geostrophic theory presented by Philip, and exploring Sánchez-Lavega et al.'s results on what can be inferred from JunoCam images. More specifically, Philip (1993)'s study, grounded in QG theory, highlights the roles of prograde vortices and potential vorticity in the behaviour of the GRS. It explores how vortices merge based on the Rossby deformation radius, how corner-like and band-like vortices differ, and how prograde vortices explain the observed behaviour of the GRS. The second study by Sánchez-Lavega et al. uses Juno spacecraft data to detail the regions within the GRS, revealing an elliptical turbulent nucleus and several other distinct cloud features surrounding it. Together, these studies deepen our understanding of Jupiter's atmosphere, providing a new perspective on one of the Solar System's greatest wonders – the Great Red Spot.

The Appendix of this report includes results of a shallow water simulation. Although the shallow water model makes assumptions that are not representative of Jupiter, such as constant density, the assumption of a shallow atmosphere, and two-dimensional behaviour, it is effective at demonstrating the interaction of multiple vortices and how they may give rise to the complicated shapes seen on Jupiter. The Jovian atmosphere is incredibly complicated, and a refined model that takes all the required variables into account is nearly impossible, so the approximations for the shallow water model are justified, as discussed in (Philip, 1993).

5 Appendix

The shallow-water model equations are linearly advective, and can be used to simulate vortices as an alternative to the QG approximation. This section will illustrate the results of a modified version of a 1-layer shallow water code developed by Tanisha Ghosal and Dr. Francis Poulin at the University of Waterloo, with the hope that it will improve our understanding of the GRS. In this report, only two vortices interacting is shown, but it's important to note that the GRS persists due to the interaction of many vortices. This code is two-dimensional, and its geometry is periodic in the x direction and channel-like in the y direction. The numerical solution is based on the pseudo-spectral method, and the Adams-Basforth method is used to approximate the solution of the ordinary differential equations (ODEs). The Coriolis parameter is defined as $f_0 = 2\Omega \sin(\theta)$, where θ can be found based on the period of the planet. For Jupiter, the day is 0.414 of an Earth day. The depth H_0 (thickness of the outer layer in which vortices occur) was estimated as 500m for Jupiter. Additionally, the time step needs to be chosen as $dt = \frac{0.2}{\sqrt{g \times h_0}} dx$ in order to resolve the dynamics. The gravity of Jupiter is $23.15 \frac{m}{s^2}$. In this case, we will initialize two vortices of opposite polarity, with one vortex being double the size of the other. The runtime is for 0.2 of a Jupiter day at a time-step of 3 seconds. The equation for the depth of these two vortices is given as:

$$h_B = -Ae^{-\frac{(x-x_{shift})^2+(y-y_{shift})^2}{(LV_1)^2}} + Be^{-\frac{(x+x_{shift})^2+(y-y_{shift})^2}{(LV_2)^2}} \quad (10)$$

Where in this case, $A = 3$, $B = 6$, $x_{shift} = -10 \text{ km}$, $y_{shift} = -20 \text{ km}$, $LV_1 = 10 \text{ km}$, and $LV_2 = 20 \text{ km}$. The vorticity plots for several instances in time are shown below.

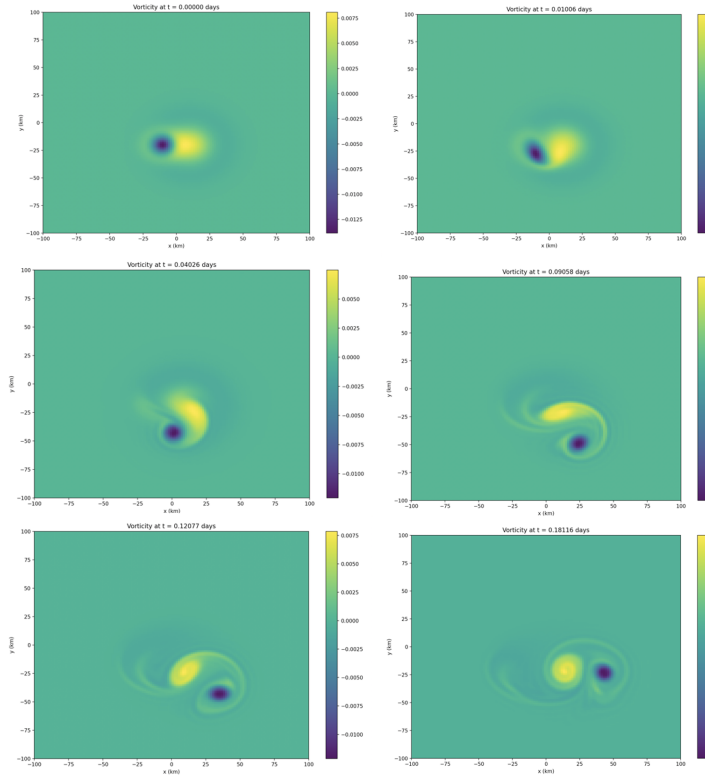


Figure 4: The vorticity (in $\frac{1}{s}$) of two opposite polarity vortices shifted by $x = 10 \text{ km}$ and $x = -10 \text{ km}$, respectively at $y = 20 \text{ km}$, with the negative vortex being double the strength of the other.

In the first frame, at $t = 0s$, the two vortices are next to one another, with the yellow spot being representative of the positive polarity vortex that is double the strength of the negative polarity vortex. As the interaction evolves in time, the dipole structure remains, and the opposite polarity of the vortices results in their spatial translation. The larger, more positive vortex moves up such that it can push down on the smaller, more negative vortex. This behaviour can be attributed to the Coriolis force, which is a result of Jupiter's rotation, causing moving objects to be deflected to the right in the northern hemisphere and to the left in the southern hemisphere. Since the

positive polarity vortex is twice as strong as the negative polarity vortex, it would experience a stronger Coriolis force. As a result, the positive vortex would tend to move towards the pole in the northern hemisphere, while the negative vortex would tend to move towards the pole in the southern hemisphere. By the Taylor-Proudman theorem, the slowly evolving flows do not vary along the direction of the rotation axis, and essentially behave like a two-dimensional flow. The flow is mainly azimuthal because of the rapid rotation, so that Coriolis accelerations balance those due to the radial pressure gradient. It's important to note that on Jupiter, the Coriolis force from the planet's rotation swirls air masses rising upwards. However, the cyclones on Earth rotate in the opposite direction from those on Jupiter. This is because on Jupiter, the vortices are formed when rising gas moves apart in the upper atmosphere. On Earth, however, they start at the bottom, where air converges and then rises. This behaviour for Jupiter is simulated in our code through the shallow water approximation, where the fluid moves at the top and the bottom layer is assumed to have no movement.

As the vortices move and interact, they shed material in their wake, known as vortex shedding. This is why there is a tail-like structure apparent in the last time frame. Next, the velocity plots in the same time frames are shown below to visualize the direction in which the vortices move. The shape in the final time frame is similar to the vortex shapes that can be seen on Jupiter, which indicates that vortices with differing polarities are a significant reason for these patterns.

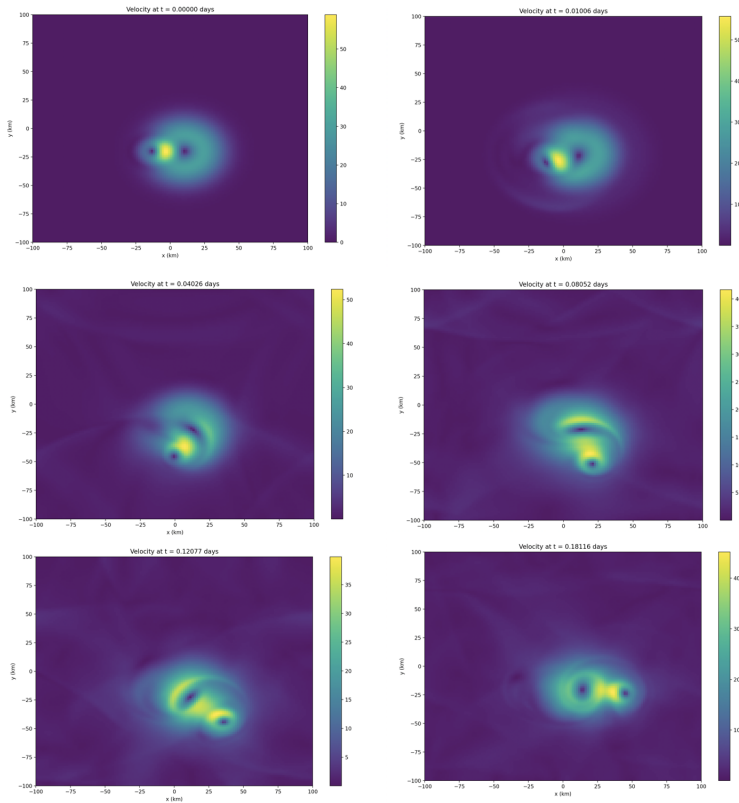


Figure 5: The velocity (in $\frac{m}{s}$) of two vortices positioned at $x = 10$ km and $y = 20$ km, with one vortex being double the strength of the other.

From these plots, it can be deduced that the larger vortex has greater velocity in its outer regions, meaning that it initially has greater speed and thereby deflects the smaller vortex. As the system evolves, the greatest velocities are in between the centres of the two vortices. Overall, the shallow water model is an effective tool to aid in the simulation of vortices, and with the inclusion of more interacting vortices, we can learn more about the dynamics seen in the GRS.

References

- [1] Sánchez-Lavega, et al. "The rich dynamics of Jupiter's great red spot from Junocam: Juno images." *The Astronomical Journal* 156.4 (2018): 162.
- [2] Marcus, P. S. (1993). Jupiter's Great Red Spot and other vortices. *Annual Review of Astronomy and Astrophysics*, 31(1), 523–569. <https://doi.org/10.1146/annurev.aa.31.090193.002515>
- [3] Achatz, U. (2022). The Dynamics of the Shallow-Water Equations. In: *Atmospheric Dynamics*. Springer Spektrum, Berlin, Heidelberg. https://doi.org/10.1007/978-3-662-63941-2_5
- [4] Ghil, M., Childress, S. (1987). Topics in Geophysical Fluid Dynamics: Atmospheric Dynamics, Dynamo Theory, and Climate Dynamics. *Applied Mathematical Sciences*, vol 60. Springer, New York, NY. https://doi.org/10.1007/978-1-4612-1052-8_8
- [5] Chorin, A.J. and Marsden, J. E. (1993) *A Mathematical Introduction to Fluid Mechanics*. Springer, New York. <http://dx.doi.org/10.1007/978-1-4612-0883-9>
- [6] Lautrup, B. (2019). *Physics of continuous matter: Exotic and everyday phenomena in the macroscopic world*. CRC Press.
- [7] Golitsyn, G. S. (1970). A similarity approach to the general circulation of planetary atmospheres. *Icarus*, 13(1), 1–24. [https://doi.org/10.1016/0019-1035\(70\)90112-0](https://doi.org/10.1016/0019-1035(70)90112-0)
- [8] Ingersoll, A. P., and P. G. Cuong, 1981: Numerical Model of Long-Lived Jovian Vortices. *J. Atmos. Sci.*, 38, 2067–2076, [https://doi.org/10.1175/1520-0469\(1981\)038j2067:NMOLLJ;2.0.CO;2](https://doi.org/10.1175/1520-0469(1981)038j2067:NMOLLJ;2.0.CO;2).
- [9] Dowling, T. E., Ingersoll, A. P. (1988). Potential Vorticity and Layer Thickness Variations in the Flow around Jupiter's Great Red Spot and White Oval BC. *Journal of Atmospheric Sciences*, 45(8), 1380-1396. [https://doi.org/10.1175/1520-0469\(1988\)045j1380:PVALTV;2.0.CO;2](https://doi.org/10.1175/1520-0469(1988)045j1380:PVALTV;2.0.CO;2)
- [10] Marcus, P. Numerical simulation of Jupiter's Great Red Spot. *Nature* 331, 693–696 (1988). <https://doi.org/10.1038/331693a0>
- [11] Rogers, J.H. (1995) *The Giant Planet Jupiter*. Cambridge University Press, Cambridge
- [12] Montgomery, M.T. and Kallenbach, R.J. (1997), A theory for vortex rossby-waves and its application to spiral bands and intensity changes in hurricanes. *Q.J.R. Meteorol. Soc.*, 123: 435-465. <https://doi.org/10.1002/qj.49712353810>
- [13] Houze, R. A. (2014). *Cloud Dynamics*, International Geophysics (Vol. 104, 432 p.). Amsterdam: Academic Press.
- [14] Tianshu Liu, Bo Wang, David S. Choi; Flow structures of Jupiter's Great Red Spot extracted by using optical flow method. *Physics of Fluids* 1 September 2012; 24 (9): 096601. <https://doi.org/10.1063/1.4752227>
- [15] Beffa, C. 2D-shallow water equations basics - applications - fluvial. (n.d.). Retrieved April 13, 2023, from https://www.fluvial.ch/m/Hydraulics2_ShallowWater_2008.pdf
- [16] Wikimedia Foundation. (2023, March 30). Great Red Spot. Wikipedia. Retrieved April 12, 2023, from https://en.wikipedia.org/wiki/Great_Red_Spot
- [17] Greicius, T. (2015, March 13). Juno Image Gallery. NASA. Retrieved April 12, 2023, from https://www.nasa.gov/mission_pages/juno/images/index.html
- [18] Scarica, P., Grassi, D., Mura, A., Adriani, A., Ingersoll, A., Li, C., et al. (2022). Stability of the Jupiter southern polar vortices inspected through vorticity using Juno/JIRAM data. *Journal of Geophysical Research: Planets*, 127, e2021JE007159. <https://doi.org/10.1029/2021JE007159>
- [19] NASA. (2022, October 17). Jupiter: In depth. NASA. Retrieved April 12, 2023, from <https://solarsystem.nasa.gov/planets/jupiter/in-depth/>
- [20] National Academies of Sciences, Engineering, and Medicine. 2011. *Vision and Voyages for Planetary Science in the Decade 2013-2022*. Washington, DC: The National Academies Press. <https://doi.org/10.17226/13117>.